Turkish Computational and Theoretical Chemistry

Turkish Comp Theo Chem (TC&TC)

Volume(Issue): 9(2) – Year: 2025 – Pages: 66-76

e-ISSN: 2602-3237

https://doi.org/10.33435/tcandtc.1507586

Received: 30.06.2024 ***Accepted:*** 13.08.2024 *Research Article*

Computational Insight into the Dual AXL/MerTK Inhibition Potential of Some AXL Inhibitors

Muhammed Tilahun Muhammed[1], Cihan Bekteş, Amine İleri

Süleyman Demirel University, Faculty of Pharmacy, Department of Pharmaceutical Chemistry, Isparta, 32000, Türkiye

Graphical abstract

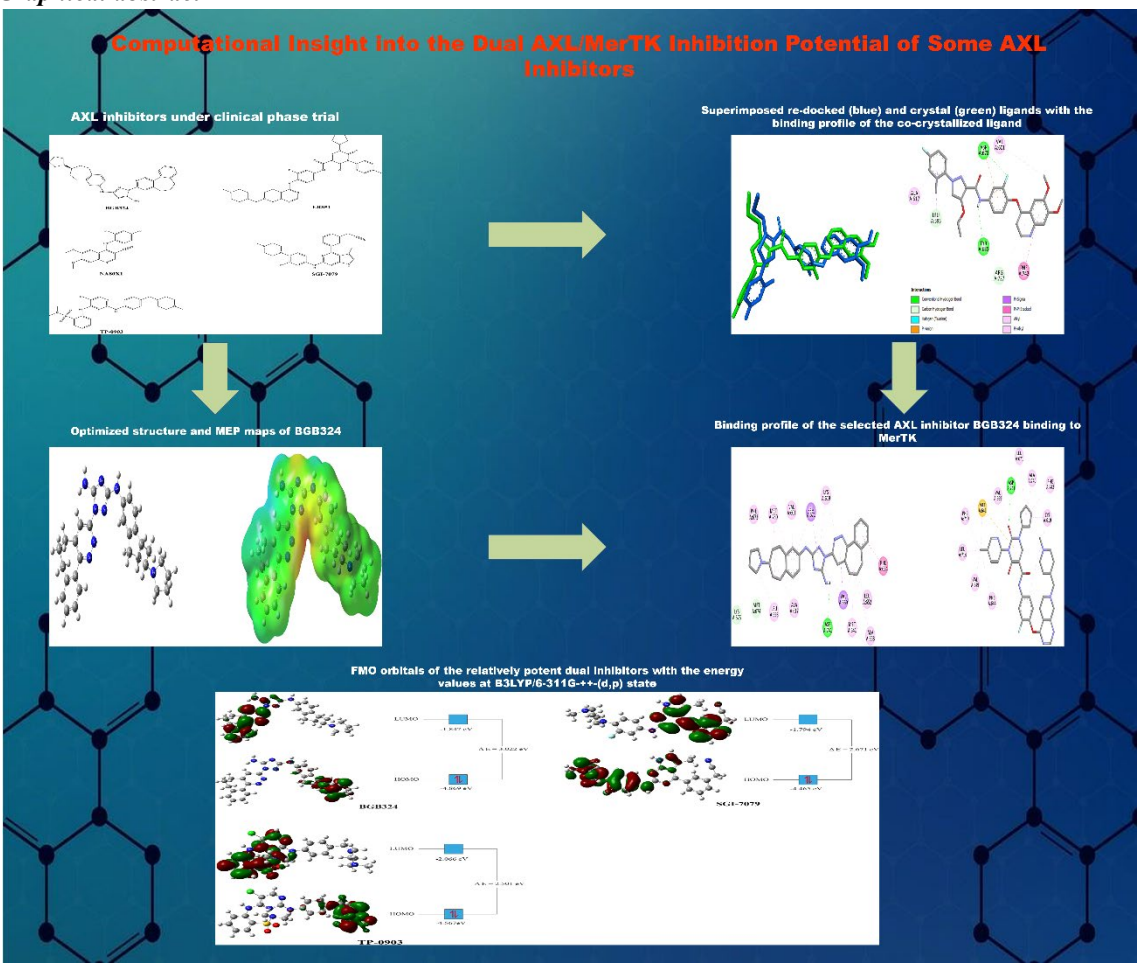

Abstract: Cancer is a multifactorial disease characterized by uncontrolled cell growth and spreading. It is still one of the leading causes of death globally. In addition to this, various side effects of the clinically available anticancer drugs and resistance developments against them have been reported. Therefore, there is an urgent need for novel drugs with high efficacy and low side effects. Tyrosine kinases are among the primary targets of research groups in this area. MerTK and AXL are members of the TAM (TYRO3, AXL, MERTK) family of receptor tyrosine kinases, which are involved in tumor cell survival, chemoresistance, and metastasis. Hence, dual inhibition of the two enzymes is an attractive target in the anticancer drug

[1] Corresponding Authors

e-mail: muh.tila@gmail.com

candidate discovery. There are efforts to discover novel chemical agents that are dual inhibitors of MerTK/AXL. In light of these findings, the inhibition potential of AXL inhibitors on MerTK was investigated through computational methods to find out their dual inhibition potency.

The binding potential of the selected AXL inhibitors to MerTK was explored through molecular docking. The docking study revealed that BGB324 might have the highest binding potential to the enzyme. Hence, BGB324 is anticipated to exhibit the highest dual inhibition among the investigated ligands. The critical structural elements of the inhibitors that would guide future lead optimizations were also determined. Furthermore, the interaction of the selected inhibitors to the enzyme via Asp741 was found to be critical in their binding. Molecular electrostatic potential and frontier molecular orbital appraisal of the selected inhibitors were also undertaken through density functional theory (DFT). The DFT study demonstrated that BGB324 would exhibit the highest chemical stability. The computational study findings need confirmation by further in vitro and in vivo studies.

Keywords: AXL, cancer, DFT, docking, MerTK

1. Introduction

Cancer is a common name for a group of diseases characterized by uncontrolled growth of cells and their spread to other tissues or organs [1]. It remains one of the leading causes of death worldwide though there are various drug therapies and treatments aimed at managing and preventing its recurrence [2]. According to the global cancer report, there were an estimated 19.3 million cancer cases and nearly 10 million cancer-related deaths worldwide in 2020. Breast cancer was the most frequently diagnosed cancer type with nearly 2,261,419 cases in the same year. On the other hand, lung cancer was the leading cause of death with nearly 1,796,144 deaths [3]. The high cancer prevalence, various side effects, and high resistance development to the drugs under clinical use need a prompt response [4]. Hence, novel drug candidates with new mechanisms are needed to combat cancer. Tyrosine kinases are among the primary targets of research groups working in the anticancer drug discovery and development area. Tyrosine kinases are a group of enzymes that play a significant role in cell signaling. They have substantial roles in cell growth, cell proliferation, cell differentiation, cell migration, apoptosis, and metabolism. Therefore, drugs targeting tyrosine kinase enzymes play an important role in cancer treatment [5,6].

MerTK and AXL are members of the TAM (TYRO3, AXL, MERTK) family of receptor tyrosine kinases (RTKs) [7]. MerTK and AXL have a direct involvement in tumor cell survival, chemoresistance, and metastasis [8]. The two also have non-overlapping functions in some cancer types. Some studies suggest dual inhibition of the two targets as this approach may result in a more potent inhibition for some cancer types. The inhibition of one may also sensitize the other one. Similarly, studies demonstrate the role of MerTK and AXL inhibitors in tumor cell inhibition and immune response modulation [9]. Their role in human autoimmune disease pathogenesis is reported and the possible role in the regulation of inflammation is also under investigation [10]. So, dual inhibition of the MerTK/AXL targets is an attractive target in the antitumor drug candidate investigation. There are efforts to discover novel chemical agents that are dual inhibitors of MerTK/AXL [11].

There are AXL inhibitors in the form of tyrosine kinase inhibitors. Various small molecule multi-target tyrosine kinase inhibitors exhibit AXL inhibition [12]. However, the AXL inhibition potency of these agents is often less effective than their potency against other kinases. Therefore, researchers focused on developing more selective AXL inhibitors. As a result, selective AXL inhibitors under various clinical phase trials are available [13,14]. BGB324 (bemcentinib), ER851, NA80X1, SGI-7079, and TP-0903 (dubermatinib) are among relatively selective AXL inhibitors under clinical phase trials (Figure 1). Recent studies pointed out the role of dual inhibition of AXL and MerTK in the discovery of potent anticancer agents as elaborated earlier [10]. The available data lead us to explore the potential of the AXL inhibitors to act as dual AXL/MerTK inhibitors. The dual inhibition potential was investigated through computational methods.

Computer-aided drug design methods are used to expedite the drug discovery and development process. Molecular docking is one such method that is widely used to expose the binding pose and binding affinity of ligands to their targets [15,16]. DFT is a quantum chemical-based computational method that is used to investigate electronic and structural properties as well as frontier molecular orbitals of compounds at different states. It is used to compare the relative stability of compounds and their reactivity [17].

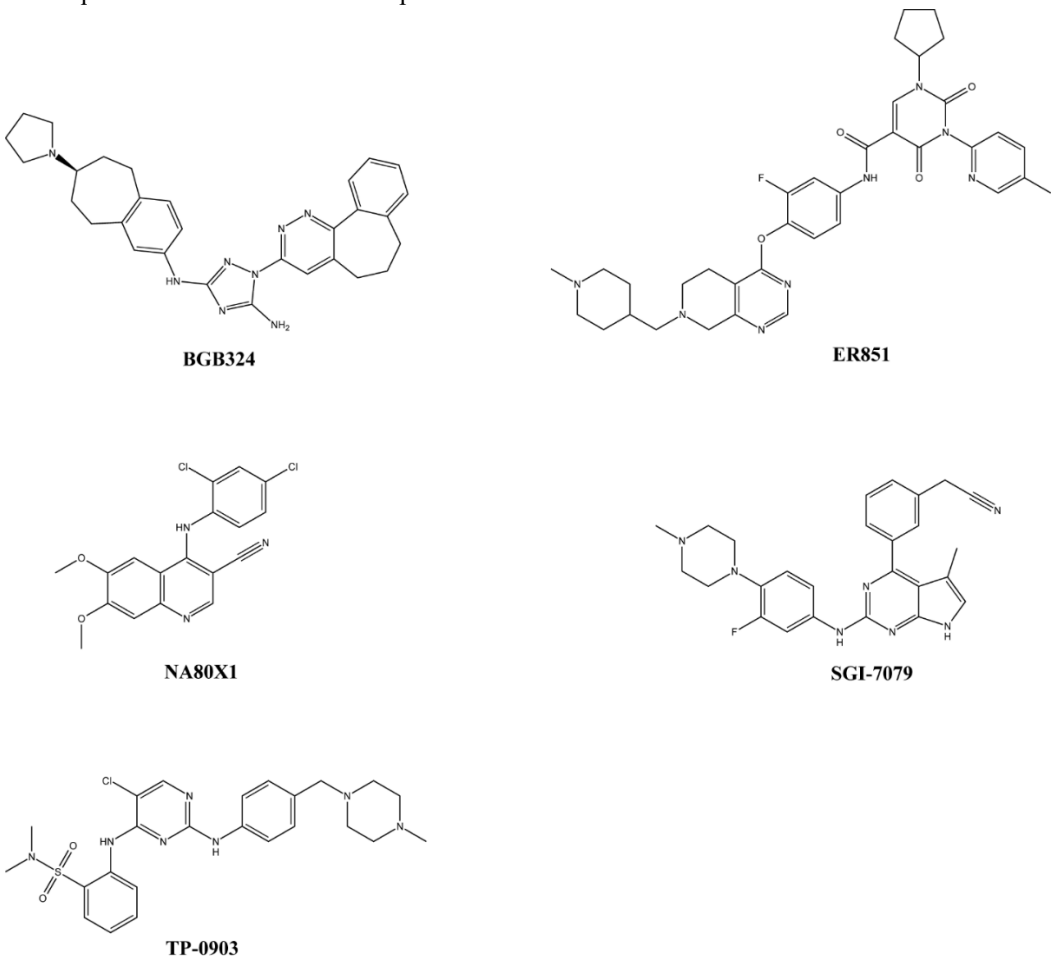

Figure 1. AXL inhibitors under clinical phase trial

The study aimed to investigate the dual AXL/MerTK inhibition potential of some selected AXL inhibitors. Five AXL inhibitors under clinical phase trial were selected to this end. A molecular docking analysis of these inhibitors against MerTK was performed to shed light on their binding potential. The docking study revealed that BGB324 had the highest binding potential to the enzyme, even higher than the native ligand. BGB324 was also anticipated to have the highest chemical stability. The binding and thus inhibition potential of BGB324 against the enzyme deserves further wet-lab analysis to confirm its dual AXL/MerTK inhibition potential.

2. Computational Method

2.1. Molecular Docking

The crystal structure of MerTK was retrieved from the RCSB PDB (Research Collaboratory for Structural Bioinformatics Protein Data Bank). The crystal structure (PDB code: 7AAX) with a resolution of 1.76 Å beard a co-crystallized ligand, LDC1267 ({N}-[4-(6,7-dimethoxyquinolin-4-yl)oxy-3-fluoranyl-phenyl]-4-ethoxy-1-(4-fluoranyl-2-methyl-phenyl)pyrazole-3-carboxamide) [18]. The ligand structures were drawn through ChemDraw and optimized through the Gaussian program [19]. The enzyme and ligands were prepared for docking as explained in the literature and the docking was done through

AutoDock Vina [20,21]. In the last step, the docking of the ligands was performed on the space in which the ligand was co-crystallized. The validation of the docking process was also undertaken by re-docking the co-crystallized ligand and making the necessary computations.

2.2. DFT Studies

The ligand structures were optimized with the Gaussian 09 program at B3LYP/6-311G++(d,p) [19]. The energy computations were then performed with the same setup at the gas phase. The HOMO (highest occupied molecular orbital) energy, LUMO (lowest unoccupied molecular orbital) energy, and the total energy of the ligands were obtained in a.u. (atomic unit). Thereafter, the related parameters were calculated after the acquired energies were converted into eV (electron volt) [22]. The values obtained were compared and analyzed. In the last step, molecular electrostatic potential (MEP) and frontier molecular orbital (FMO) analysis were undertaken after visualization was performed with GaussView 5.0 [23].

3. Results and Discussion

3.1. Molecular Docking

The docking process was validated by re-docking the co-crystallized ligand first. For this purpose, the crystal ligand and the re-docked ligand were superimposed to compute the RMSD (root mean square deviation). The RMSD value between the two structures was found to be 1.3474 Å (Figure 2). This value is below the threshold RMSD value for reliable docking (2 Å) [15]. Hence, the re-docked ligand was settled in a common space with the co-crystallized ligand. As a result, it is expected to interact through similar amino acid residues. This premise was examined by comparing the binding residues of the co-crystallized ligand in the docking and the reported crystallographic studies. The crystallographic study revealed that various selective and dual inhibitors interacted with MerTK through a limited number of amino acid residues. The investigated inhibitors had interactions through Phe742. In this docking, the co-crystallized ligand had interactions via Phe742. Thus, the residue that was reported to be critical in the interaction of the inhibitors with the enzyme was met. The interaction of the co-crystallized ligand with the enzyme was achieved through the involvement of diverse amino acid residues (Table 1, Figure 2). Thus, the binding residues were evaluated based on the reported studies that consisted of docking of MerTK. A computational study reported the interaction of compounds with MerTK through various residues including via Leu593 [24]. Another computational study reported the interaction of compounds to the enzyme through residues including Val601, Tyr685, and Arg727 [25]. A computational study reported the interaction of various ligands with the enzyme. In this study, the ligands interacted with the enzyme via diverse residues including Leu593, Val601, Ala617, Asp678, and Arg727 residues [26]. So, all the binding residues of the co-crystallized ligand were observed in the reported computational studies. The high degree of interaction residue similarity with the reported experimental and computational studies proved that the choice of the binding box in the docking was good enough to give reliable results. In short, the low RMSD value detected and the high residual similarity with the available literature implied a reliable docking procedure.

Some of the selective AXL inhibitors had a higher MerTK inhibition potential than the co-crystallized ligand. The co-crystallized ligand is a MerTK inhibitor [18]. Thus, it was utilized as a benchmark to measure the binding potential of the selective AXL inhibitors. The binding affinities of BGB324, SGI-7079, and TP-0903 were found to be higher than that of the co-crystallized ligand. These inhibitors gave a binding affinity lower than -10 kcal/mol (Table 1). Hence, they are anticipated to have relatively higher binding affinity towards the enzyme. BGB324 and SGI-7079 formed just a conventional hydrogen bond with the enzyme as the other two inhibitors. Nevertheless, BGB324 had twenty-one more interactions with the enzyme. Similarly, SGI-7079 had seventeen more other interactions with the enzyme. On the other hand, ER851 and NA80X1 formed thirteen and twelve other interactions with the enzyme (Table 1, Figure 3). Hence, BGB324 and SGI-7079 are expected to have stronger interactions with the enzyme as they form much more non-conventional hydrogen bond interactions. TP-0903 is also expected to have an interaction near the two inhibitors with relatively stronger interactions. Because it had three conventional hydrogen bonds with the enzyme. Conventional hydrogen bonding is crucial in the

binding of a ligand to a target and keeping it stable inside the binding site [4]. So, it is expected to have a comparable interaction strength with the inhibitors with better interaction potential. Together with this, it is expected to form weaker interactions than the two compounds as it formed just five other interactions with the enzyme (Table 1, Figure 3).

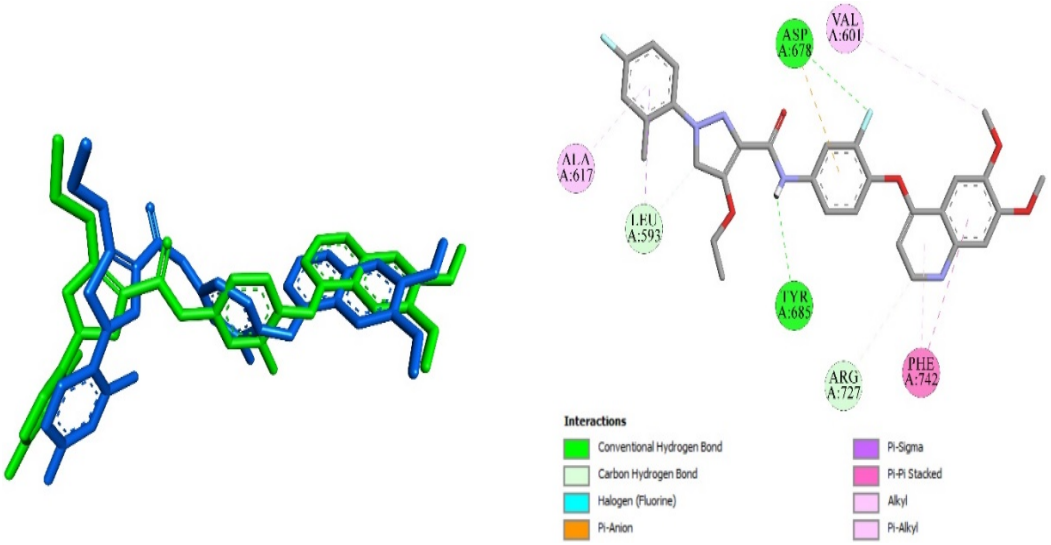

Superimposed ligands Binding profile

Figure 2. Superimposed re-docked (blue) and crystal (green) ligands with the binding profile of the co-crystallized ligand

The co-crystallized ligand formed two conventional hydrogen bonds with the enzyme. Though BGB324 and SGI-7079 formed a conventional hydrogen bond with the enzyme, they had much higher other types of interaction than the co-crystallized ligand. The hydrogen bond of BGB324 had a distance of 2.36 Å. Similarly, the hydrogen bond distance of SGI-7079 was found to be 2.80 Å. On the other hand, the hydrogen bond distances of TP-0903 were 2.33 Å (with Asp678), 2.73 Å (with Lys675), and 2.84 Å (with Met674). The bond distance of the hydrogen bond through Asp678 was close to the distance of the BGB324 hydrogen bond. The other two hydrogen bonds would have less effect in bringing the binding as their distance was higher [27,28]. The hydrogen bond distance for the native ligand was 2.41 Å for Tyr685 and 2.71 Å for Asp678. The hydrogen bond with Tyr685 is anticipated to play a higher role in the binding of the ligand. The hydrogen bond distance analysis revealed that some of them are far, which might result in a lower binding strength contribution for them. In such cases, the contribution of other types of interactions will be important. The docking study exhibited that BGB324 and SGI-7079 formed a much higher number of interactions that would compensate for or in some cases overpass the higher hydrogen bonds formed with TP-0903. Therefore, they are expected to have a stronger interaction than the rest two compounds with the enzyme. In short, BGB324, SGI-7079, and TP-0903 would exhibit a higher binding potential to the enzyme relative to the native ligand. With this being noted, BGB324 is anticipated to have the highest binding potential to MerTK among the AXL inhibitors due to its high binding affinity to the enzyme.

Table 1. Binding affinities and residues of the selected AXL inhibitors in their interaction with MerTK

Compounds	Binding affinity (kcal/mol)	Conventional hydrogen bonding points	Other interaction points
BGB324	-10.9	Asp741	Leu593(2)[a], Val601[b], Ala617[a], Ala617[b], Lys619(2)[b], Phe634[c], Ala638[a], Met641[a], Leu652[a], Val669[a], Val669[b], Val669[d], Leu671[b], Leu671[d], Phe673[a], Met674[e], Lys675[e], Met730[a], Met730[b]

ER851	-9.5	Asp741	Phe598[e], Lys619[a], Lys619[b], Met641[a], Met641[f], Phe644[a], Val649[a], Val669[b], Leu671[a], Leu714[a], Phe719[a], Ala740[a], Phe742[a]
NA80X1	-8.0	Asp741	Met621[a], Phe634[a], Met641(2)[a], Met641[f], Phe644[a], Val649[a], Ile650[a], Leu652[a], Val669[d], Leu714[a], Phe719[a]
SGI-7079	-10.7	Asp741	Leu593(2)[b], Val601(2)[b], Val601[d], Ala617(2)[b], Ala617[d], Lys619[b], Leu671[b], Phe673[c], Asp678[g], Arg727[a], Met730[d], Met730[f], Phe742[c], Phe742[d]
TP-0903	-10.1	Met674, Lys675, Asp678	Leu593[b], Leu593[e], Gly677[e], Thr690(2)[e], Pro692[b]
Ligand	-9.7	Asp678, Tyr685	Leu593[d], Leu593[e], Val601[a], Ala617[b], Asp678[h], Asp678[g], Arg727[e], Phe742[b], Phe742[c]

[a]alkyl, [b]pi-alkyl, [c]pi-pi, [d]pi-sigma, [e]carbon-hydrogen bond, [f]pi-sulfur, [g]halogen, [h]pi-ion

In the docking study, the AXL inhibitors interacted with the enzyme through common amino acid residues. Together with this, some of the TP-0903 interaction residues were different from the interaction residues of the rest inhibitors. The interaction of the inhibitors via Asp741 residue was found to be critical as four of them had a conventional hydrogen bond. A previous study reported that the interaction through Asp741 was critical in the binding of a ligand to MerTK [25]. Therefore, the finding of the docking study was in line with the study. The interaction residues of the AXL inhibitors obtained from the docking study were similar with the results of the computational studies in the literature. The interaction residues of TP-0903 were somewhat different from the rest AXL inhibitors. Its interaction through Leu593 was observed in the interaction of the other inhibitors and the reported computational studies. On the other hand, its interaction through Asp678 was observed in the interaction of the co-crystallized ligand and the reported computational studies. A computational study reported the interaction of tomentosin with the enzyme via Met674. Another computational study reported conventional hydrogen bonding of theanine with the enzyme. The same study reported the interaction of vanillic via Gly677 [26]. Hence, the interaction residues of TP-0903, except the one via Thr690 and Pro692, were observed in the previous computational studies. The interaction residues of BGB324, ER851, NA80X1, and SGI-7079 were common in the reported studies [24–26,29,30]. In short, the findings of the docking study were in line with the literature.

The docking analysis revealed that some of the AXL inhibitors had higher binding potential to MerTK than the native ligand. BGB324 had the highest binding potential to the enzyme. Hence, BGB324 might be a dual inhibitor of the AXL/MerTK enzymes. The findings of the study need further approval by extending them to wet lab studies. Together with this, the docking study will serve as a basis for designing dual AXL/MerTK with a similar scaffold to the selective AXL inhibitors. The selected AXL inhibitors had diverse structural elements. As a result, it is hard to infer a direct structure-activity relation from the result. Together with this, the hydrogen on the nitrogens of some of the AXL inhibitors and the native ligand acted as a hydrogen bond donor. Some others formed hydrogen bonding with a hydrogen bond acceptor, nitrogen and oxygen (Figure 3). Especially, the nitrogen of the cyanide group in NA80X1 and SGI-7079 played a crucial role in hydrogen bond formation. It is recommended to preserve the amino substituent of the triazole heterocyclic ring in the structure of BGB324 in future lead optimization of the ligand for dual inhibition.

3.2. DFT Studies

The DFT calculations of the ligands with the highest binding potential to MerTK, BGB324, SGI-7079, and TP-0903, were performed. After the DFT calculations were made, MEP appraisal and FMO analysis were performed separately.

3.2.1. Molecular Electrostatic Potential Appraisal

The MEP maps of BGB324, SGI-7079, and TP-0903 were sketched from the DFT computations to get an insight into electrophilic and nucleophilic region distributions. Nucleophilic reactivity parts of a compound are represented by predominantly blue regions whereas electrophilic reactivity parts of a compound are represented by predominantly red or yellow (to some level) regions [31]. One of the

nitrogens of the triazole heterocyclic ring in the BGB324 structure was near the mainly red-like vicinity. Similarly, one of the hydrogens of the phenyl ring tethered to the amine functional group was directed to the yellow vicinity (Figure 3). The SGI-7079 gave predominantly red vicinities around the nitrogen of acetonitrile and pyrimidin-4-yl. One of the hydrogens and the fluorine of the fluoro-substituted phenyl were also close to the yellow vicinities (Figure 4). In the TP-0903 structure, a predominantly red vicinity was observed around the oxygen in the sulfonate group (Figure 4). The above-listed structural elements might contribute to the electrophilic reactivity of the compounds. On the other hand, the hydrogens of the two amine groups, the pyridazin-3-yl, and the cyclohepta in the BGB324 structure were mainly near the blue vicinity (Figure 4). Similarly, the hydrogens of the aceto, pyrrole, and the amine bridge of SGI-7079 were mainly surrounded by blue vicinities (Figure 4). Some of the hydrogens of sulfonamide-substituted phenyl were surrounded by predominantly yellow vicinity (Figure 4). The listed structural elements might contribute to the nucleophilic reactivity of the respective ligands. The MEP analysis demonstrated that the likely structural components that would contribute to the electrophilic reactivity mainly resulted from electronegative atoms. On the other hand, the hydrogens of the ligands contributed highly to the nucleophilic reactivity as expected. Some exceptional results were also observed in the provided figures. Such results are obtained in two-dimensional figures that might sometimes give the due results to the atomic properties in the three-dimensional detail analysis.

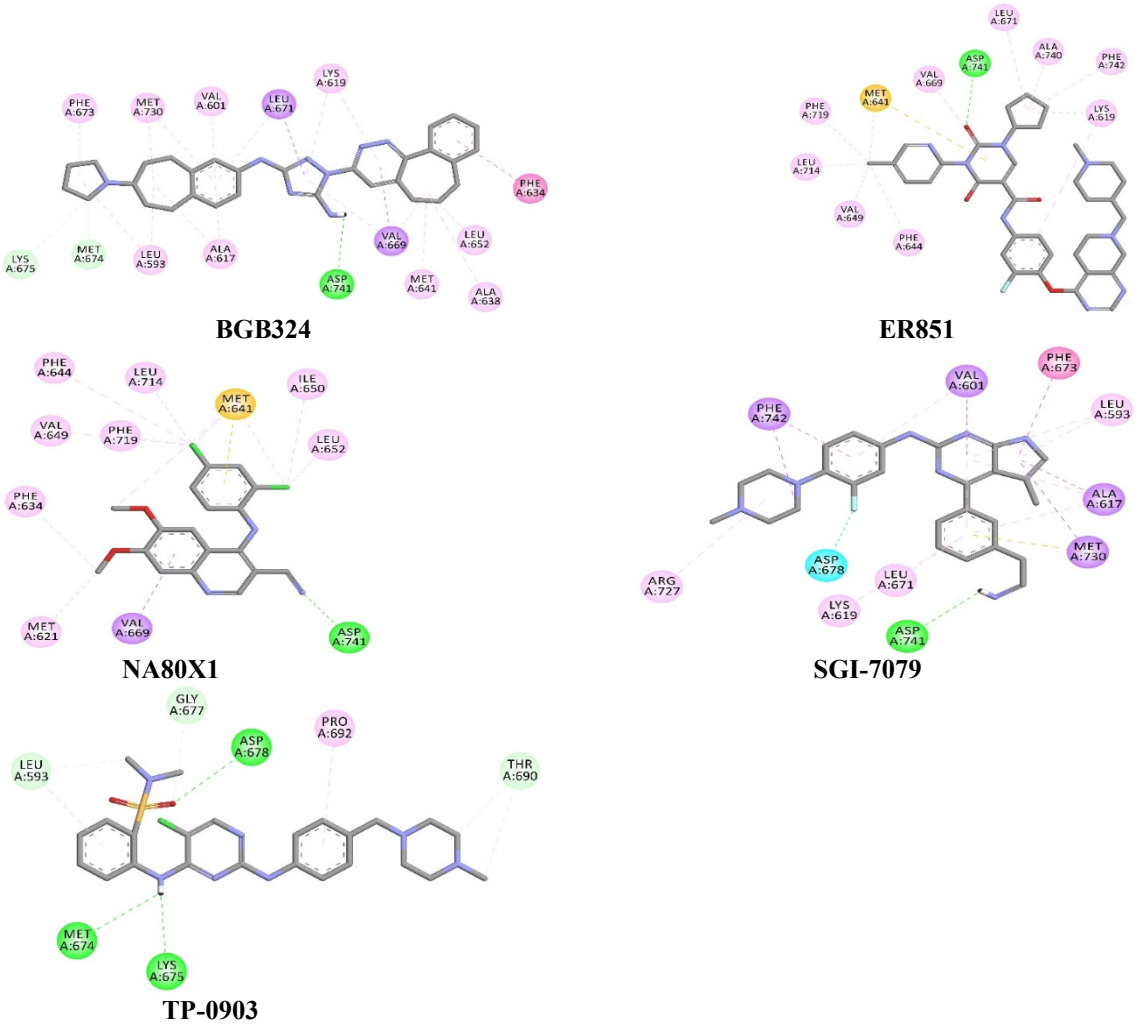

Figure 3. Binding profile of the selected AXL inhibitors in their binding to MerTK

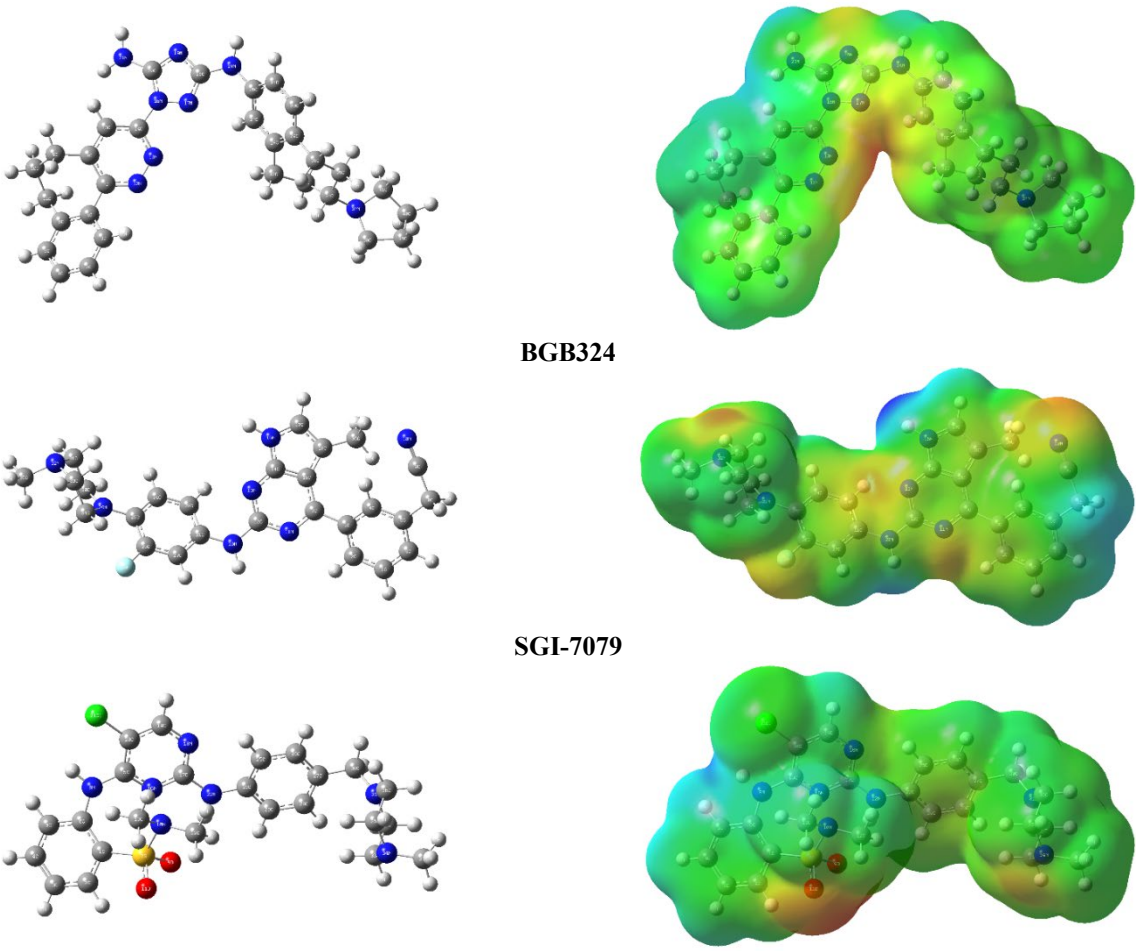

BGB324

SGI-7079

TP-0903

Figure 4. Optimized structure and MEP maps of BGB324, SGI-7079, and TP-0903

Table 2. HOMO energies, LUMO energies, and related parameters (in eV)

Parameters	BGB324	SGI-7079	TP-0903
E_{total}	-43,575.5	-40,524.7	-63,245.3
E_{HOMO}	-4.869	-4.465	-4.567
E_{LUMO}	-1.847	-1.794	-2.066
ΔE	3.022	2.671	2.501
Ionization potential ($IP= -E_{HOMO}$)	4.869	4.465	4.567
Electron affinity ($A = -E_{LUMO}$)	1.847	1.794	2.066
Chemical potential ($\mu = -(I + A)/2$)	-3.358	-3.130	-3.317
Hardness ($\eta = (I-A)/2$)	1.511	1.336	1.251
Mulliken electronegativity ($\chi = (I + A)/2$) [34]	3.358	3.130	3.317
Softness ($S = 1/2\eta$)	0.331	0.374	0.400
Electrophilicity index ($\omega = \mu^2/2\eta$) [35]	3.732	3.664	4.401
Maximum charge transfer ($\Delta N_{max}= (I+A)/2(I-A)$) [36]	1.111	1.171	1.326

3.2.2. Frontier Molecular Orbital Analysis

The FMO analysis of the three ligands was performed to grasp their general electrical properties. The electron exchange capacity of the ligands and their relative stability were measured by using the HOMO-LUMO energies and energy gap (ΔE). HOMO energy is linked to the electron-donating capacity of compounds. A higher HOMO energy implies a higher electron-donating capacity [32]. From the analyzed ligands, SGI-7079 is anticipated to exhibit the highest capacity to give electrons as its HOMO energy was the highest. On the other hand, the LUMO energy was linked to the electron-accepting capacity of compounds. A

higher LUMO energy implies a higher electron-accepting capacity. SGI-7079 gave the highest LUMO energy implying the highest electron-accepting capacity for it (Table 2). Thus, SGI-7079 is expected to exhibit the highest electron exchange capacity among the investigated ligands. The energy gap between the LUMO and the HOMO energies is linked to the chemical stability of compounds. A higher energy gap implies a higher chemical stability for a compound [33]. BGB324 is anticipated to show the highest chemical stability according to the DFT results. The highest hardness among the investigated ligands belongs to BGB324 (Table 2). Hence, BGB324 is expected to exhibit the highest chemical stability and the least reactivity.

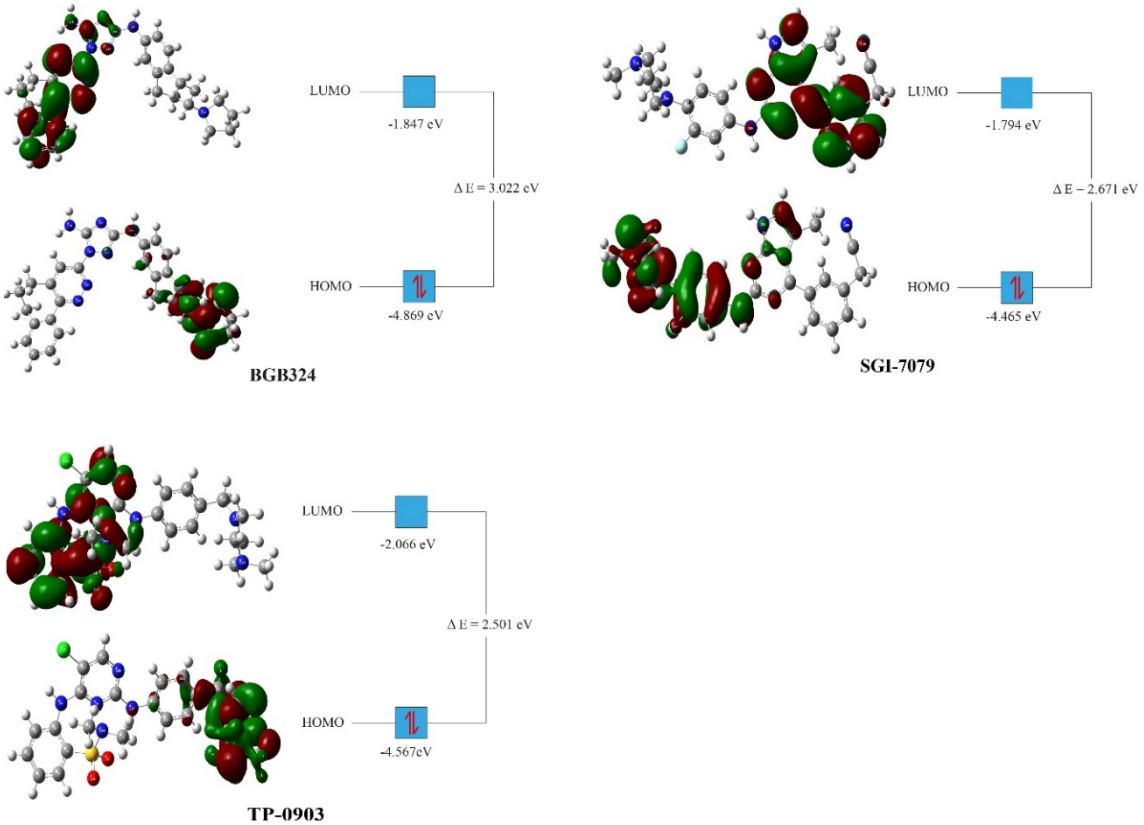

Figure 5. FMO orbitals of the relatively potent dual inhibitors with the energy values at B3LYP/6-311G++(d,p) state

4. Conclusions

Some AXL inhibitors under clinical phase trials were selected by doing a literature review. The potential of these inhibitors to bind and thus inhibit MerTK was explored through molecular docking. The computational study aimed to find out the dual inhibition potential of the selected inhibitors. The docking study showed that BGB324, SGI-7079, and TP-0903 slightly had higher binding potential than the native ligand. Particularly, BGB324 had the highest binding potential to the enzyme as it had the highest binding affinity. BGB324 was found to interact with the enzyme through similar residues detected in the reported studies. Most of the hydrogen bonds were formed with the involvement of either the amine or the cyanide groups of the inhibitor compounds. The amino substituent of the BGB324 was responsible for hydrogen bond formation in the docking. Hence, preserving the amino substituent is recommended in future lead optimization endeavors toward developing dual AXL/MerTK inhibitors. In addition to this, a DFT study was undertaken to figure out the structural, electrical, and FMO properties of the ligands. The DFT study showed that BGB324 would exhibit the highest chemical stability among the investigated inhibitors. To wrap up, the computational study results would guide researchers to design dual AXL/MerTK inhibitors with high efficacy.

ACKNOWLEDGEMENT

The numerical calculations reported in this paper were partially performed at TUBITAK ULAKBIM, High Performance and Grid Computing Center (TRUBA resources).

References

[1] M.R. Stratton, P.J. Campbell, P.A. Futreal, The cancer genome, Nat. 2009 4587239. 458 (2009) 719–724.

[2] F. Bray, M. Laversanne, E. Weiderpass, I. Soerjomataram, The ever-increasing importance of cancer as a leading cause of premature death worldwide, Cancer. 127 (2021) 3029–3030.

[3] H. Sung, J. Ferlay, R.L. Siegel, M. Laversanne, I. Soerjomataram, A. Jemal, F. Bray, Global Cancer Statistics 2020: GLOBOCAN Estimates of Incidence and Mortality Worldwide for 36 Cancers in 185 Countries, CA. Cancer J. Clin. 71 (2021) 209–249.

[4] M.T. Muhammed, Z. Kokbudak, S. Akkoc, Cytotoxic activities of the pyrimidine-based acetamide and isophthalimide derivatives: an in vitro and in silico studies, Mol. Simul. (2023) 1–11.

[5] J.D. Paccez, M. Vogelsang, M.I. Parker, L.F. Zerbini, The receptor tyrosine kinase Axl in cancer: Biological functions and therapeutic implications, Int. J. Cancer. 134 (2014) 1024–1033.

[6] C. Zhu, Y. Wei, X. Wei, AXL receptor tyrosine kinase as a promising anti-cancer approach: functions, molecular mechanisms and clinical applications, Mol. Cancer 2019 181. 18 (2019) 1–22.

[7] A.L. Prieto, C. Lai, The TAM Subfamily of Receptor Tyrosine Kinases: The Early Years, Int. J. Mol. Sci. 25 (2024) 116475.

[8] R.M.A. Linger, R.A. Cohen, C.T. Cummings, S. Sather, J. Migdall-Wilson, D.H.G. Middleton, X. Lu, A.E. Barón, W.A. Franklin, D.T. Merrick, P. Jedlicka, D. Deryckere, L.E. Heasley, D.K. Graham, Mer or Axl receptor tyrosine kinase inhibition promotes apoptosis, blocks growth and enhances chemosensitivity of human non-small cell lung cancer, Oncogene 2013 3229. 32 (2012) 3420–3431.

[9] J.M. Huelse, D.M. Fridlyand, S. Earp, D. DeRyckere, D.K. Graham, MERTK in cancer therapy: Targeting the receptor tyrosine kinase in tumor cells and the immune system, Pharmacol. Ther. 213 (2020) 107577.

[10] A. Nerviani, M.A. Boutet, G.M. Ghirardi, K. Goldmann, E. Sciacca, F. Rivellese, E. Pontarini, E. Prediletto, F. Abatecola, M. Caliste, S. Pagani, D. Mauro, M. Bellan, C. Cubuk, R. Lau, S.E. Church, B.M. Hudson, F. Humby, M. Bombardieri, M.J. Lewis, C. Pitzalis, Axl and MerTK regulate synovial inflammation and are modulated by IL-6 inhibition in rheumatoid arthritis, Nat. Commun. 15 (2024) 2398.

[11] D. Kong, Q. Tian, Z. Chen, H. Zheng, M.A. Stashko, D. Yan, H.S. Earp, S. V. Frye, D. DeRyckere, D. Kireev, D.K. Graham, X. Wang, Discovery of Novel Macrocyclic MERTK/AXL Dual Inhibitors, J. Med. Chem. 67 (2024) 5866–5882.

[12] Z. Liu, L. Chen, J. Zhang, J. Yang, X. Xiao, L. Shan, W. Mao, Recent discovery and development of AXL inhibitors as antitumor agents, Eur. J. Med. Chem. 272 (2024) 116475.

[13] S. Bhalla, D.E. Gerber, AXL Inhibitors: Status of Clinical Development, Curr. Oncol. Rep. 25 (2023) 521–529.

[14] N. Ebrahimi, E. Fardi, H. Ghaderi, S. Palizdar, R. Khorram, R. Vafadar, M. Ghanaatian, F. Rezaei-Tazangi, P. Baziyar, A. Ahmadi, M.R. Hamblin, A.R. Aref, Receptor tyrosine kinase inhibitors in cancer, Cell. Mol. Life Sci. 80 (2023).

[15] M.T. Muhammed, E. Aki-Yalcin, Molecular Docking: Principles, Advances, and its Applications in Drug Discovery, Lett. Drug Des. Discov. 21 (2024) 480–495.

[16] M.T. Muhammed, E. Aki-Yalcin, Pharmacophore modeling in drug discovery: methodology and current status, J. Turkish Chem. Soc. Sect. A Chem. 8 (2021) 759–772.

[17] S. Khatun, R.P. Bhagat, S.A. Amin, T. Jha, S. Gayen, Density functional theory (DFT) studies in HDAC-based chemotherapeutics: Current findings, case studies and future perspectives, Comput. Biol. Med. 175 (2024) 108468.

[18] A. Pflug, M. Schimpl, J.W.M. Nissink, R.C. Overman, P.B. Rawlins, C. Truman, E. Underwood, J. Warwicker, J. Winter-Holt,

W. McCoull, A-loop interactions in Mer tyrosine kinase give rise to inhibitors with two-step mechanism and long residence time of binding, Biochem. J. 477 (2020) 4443–4452.

[19] M.J. Frisch, G.W. Trucks, H.B. Schlegel, G.E. Scuseria, M.A. Robb, J.R. Cheeseman, G. Scalmani, V. Barone, G.A. Petersson, H. Nakatsuji, X. Li, M. Caricato, A. Marenich, J. Bloino, B.G. Janesko, R. Gomperts, B. Mennucci, H.P. Hratchian, J. V. Ort, D.J. Fox, Gaussian 09, (2009) 53–54.

[20] O. Trott, A.J. Olson, AutoDock Vina: improving the speed and accuracy of docking with a new scoring function, efficient optimization and multithreading, J. Comput. Chem. 31 (2010) 455.

[21] B. Gökçe, M.T. Muhammed, Evaluation of in vitro effect, molecular docking, and molecular dynamics simulations of some dihydropyridine-class calcium channel blockers on human serum paraoxonase 1 (hPON1) enzyme activity, Biotechnol. Appl. Biochem. (2023).

[22] A.M. Senan, M.T. Muhammed, L.A. Al-Shuraym, S.K. Alhag, N.A.S. Al-Areqi, S. Akkoç, Synthesis, structure characterization, DFT calculations, and computational anticancer activity investigations of 1-phenyl ethanol derivatives, J. Mol. Struct. 1294 (2023) 136323.

[23] J.M. Dennington, R.D., Keith, T.A. Millam, GaussView 5.0, (2008).

[24] Z. Yu, X. Li, C. Ge, H. Si, L. Cui, H. Gao, Y. Duan, H. Zhai, 3D-QSAR modeling and molecular docking study on Mer kinase inhibitors of pyridine-substituted pyrimidines, Mol. Divers. 19 (2015) 135–147.

[25] S.P. Bhujbal, S. Keretsu, P.K. Balasubramanian, S. Joo, Macrocyclic effect on inhibitory activity : a modeling study on MerTK inhibitors, Med. Chem. Res. 28 (2019) 1923–1938.

[26] D.J. Lambo, C.G. Lebedenko, P.A. Mccallum, I.A. Banerjee, Molecular dynamics , MMGBSA , and docking studies of natural products conjugated to tumor - targeted peptide for targeting BRAF V600E and MERTK receptors, Springer International Publishing, 2023.

[27] H. Mehmood, T. Akhtar, M. Haroon, M. Shah, U. Rashid, S. Woodward, Synthesis of Hydrazinylthiazole Carboxylates: A Mechanistic Approach for Treatment of Diabetes and Its Complications, Future Med. Chem. 15 (2023) 1149–1165.

[28] H. Mehmood, M. Haroon, T. Akhtar, S. Woodward, S. Haq, S. M Alshehri, Synthesis, anti-diabetic profiling and molecular docking studies of 2-(2-arylidenehydrazinyl)thiazol-4(5H)-ones, Future Med. Chem. 16 (2024) 1255–1266.

[29] T. Qin, M. Hasnat, Y. Zhou, Z. Yuan, W. Zhang, Macrophage malfunction in Triptolide-induced indirect hepatotoxicity, (2022) 1–14.

[30] Y. Di, Y. Bao, Z. Zhu, S. Sun, F. Tian, F. Wang, G. Yu, M. Zhang, J. Han, L. Zhou, Tomentosin suppressed M1 polarization via increasing MERTK activation mediated by regulation of GAS6, J. Ethnopharmacol. 314 (2023) 116429.

[31] M. Mavvaji, M.T. Muhammed, S. Akkoc, Synthesis, Cytotoxic Activity, Docking and MD Simulation of N,N-Disubstituted New Benzimidazolium Salts, ChemistrySelect. 8 (2023) e202303053.

[32] N.K. Kınaytürk, E. Önem, H. Oturak, Benzoic acid derivatives: Anti-biofilm activity in Pseudomonas aeruginosa PAO1, quantum chemical calculations by DFT and molecular docking study, Bull. Chem. Soc. Ethiop. 37 (2023) 171–181.

[33] N.K. Kinaytürk, Spectroscopic Characterization, DFT Calculation, and Docking Analysis for Understanding Molecular Interaction Mechanism of Propiconazole and DNA, J. Appl. Spectrosc. 90 (2024) 1334–1345.

[34] R.G. Parr, R.A. Donnelly, M. Levy, W.E. Palke, Electronegativity: The density functional viewpoint, J. Chem. Phys. 68 (1978) 3801.

[35] P.K. Chattaraj, U. Sarkar, D.R. Roy, Electrophilicity index, Chem. Rev. 106 (2006) 2065–2091.

[36] T. Koopmans, About the assignment of wave functions and eigenvalues to the individual electrons of an atom, Physica. 1 (1934) 104–113.